NASA Technical Memorandum 86399

MEASUREMENTS IN THE FLOW FIELD OF A CYLINDER WITH A LASER TRANSIT ANEMOMETER AND A DRAG RAKE IN THE LANGLEY 0.3 m TRANSONIC CRYOGENIC TUNNEL

WILLIAM C. HONAKER AND PIERCE L. LAWING

(NASA-TM-86399) MEASUREMENTS IN THE FLOW FIELD OF A CYLINDER WITH A LASER TRANSIT ANEMOMETER AND A DRAG RAKE IN THE LANGLEY 0.3 m TRANSONIC CRYOGENIC TUNNEL (NASA) 25 p HC A02/MF A01 CSCL 14B G3/35

N85-24270

Unclas 14871

APRIL 1985

National Aeronautics and Space Administration

Langley Research Center
Hampton, Virginia 23665

SUMMARY

An experiment was conducted at the 0.3 m Transonic Cryogenic Tunnel using a Laser Transit Anemometer (LTA) to probe the flow field around a 3.05 centimeter-diameter circular cylinder. Measurements were made along the stagnation line and determination of particle size was evaluated by their ability to follow the flow field. The LTA system was also used to scan into the boundary layer near the 45 degree point on the model. Results of these scans are presented in graphic and tabular form. Flow field particle seeding was accomplished by inbleeding dry service air. The residual moisture (5-10 ppm) condensed and formed ice particles which served as Mie scattering centers for the LTA detection system. Comparison of data taken along the stagnation streamline with theory indicated that these particles tracked the velocity gradient of the flow. Tunnel operating conditions for the tests were a Mach number of 0.3, a pressure of 1.93×10^5 n/m^2, and a temperature of 225 degrees K. Free stream Mach number and pressure were varied for the particle size determination.

INTRODUCTION

In aerodynamics flow fields, it is always highly desirable to measure fluid parameters nonintrusively. Laser anemometry, which requires only a few milliwatt laser beam to probe the test medium, offers a method of evaluating free stream velocity, flow angle, turbulence intensity and shear stress. The laser beam can be scanned along each of three orthogonal axes by an appropriate electro-optical package located outside of the flow to provide complete flow field maps. Since the device operates in the backscatter mode, it also allows the determination of the flow field at wing or turbine blade junctures to provide information on complex 3-D flow fields.

Applying optical techniques in the hostile environments of cryogenic wind tunnels often entails special engineering considerations. In large wind tunnels it would be desirable to house the system within the plenum where it would be necessary to protect it from low temperature and high pressure. In small wind tunnels there is insufficient room in the plenum for a system the size of the Laser Transit Anemometer (LTA), and other problems such as viewing through pressure shell windows, which must simultaneously accommodate large temperature and pressure gradients, also have to be addressed. Also, fundamental problems of seeding and measurement accuracy in cryogenic flows remain unresolved and are currently being investigated in the Langley Research Center 0.3 m Transonic Cryogenic Tunnel (TCT). A 3.048-cm diameter circular cylinder was used in this study to provide a reasonably simple model with which to compare experimental data and theory.

During an earlier entry into the 0.3 m TCT with the LTA system, measurements had been made across a standing shock on an airfoil and the particle size and concentration had been estimated (refs. 1-3). However, subsequent inspection indicated that the particles were produced by an oil leak from the fan drive shaft, raising the question of whether there was any natural seeding available.

The goals for the present experiment were: (1) evaluate the natural seeding in the 0.3 m TCT to determine if the natural particulate concentration was sufficiently high to make meaningful LTA flow field measurements; (2) make stagnation line surveys and estimate particle size; (3) make exploratory scans into the boundary layer to determine the LTA's capability to operate in this region; and (4) keep the optical access to the tunnel test section clear of condensation and frost.

SYMBOLS

α	mean flow angle (degrees)
b	background (counts)
C_D	drag coefficient
d	distance between laser beams, spots (μm)
D	cylinder diameter (cm)
h	value of peak store of histogram (counts)
M_∞	free stream Mach number
p	pressure (newtons/meter^2)
p_∞	free stream static pressure (psi)
p_t	total pressure (newtons/meter^2)
rpm	revolutions per minute
R_e	free stream Reynolds number (1/ft)
R_D	Reynolds number based on cylinder diameter
t	time
V_∞	free stream velocity (m/sec)
V	mean velocity (m/sec)
x	distance along stagnation line to cylinder surface (cm)

DESCRIPTION OF EXPERIMENTAL APPARATUS

Laser Transit Anemometer (LTA)

LTA was developed to handle applications (e.g., within turbomachinery) where conventional Laser Doppler Velocimetry (LDV) was difficult to apply. The technique is described in reference 4. The LTA measures the transit time of particles that cross two focused laser beams. The optical package sketched in figure 1 forms "two spots" in space and detects light scattered from particles passing through them. The detected signals are correlated in time and this autocorrelation allows an estimate of the average transit time, t. This average transit time in conjunction with the known spot separation, d, provides a measurement of the velocity, V, of the particle by

$$V = d/t.$$

LTA system control, data acquisition and data processing is performed by a microprocessor based computer system.

The optics package (fig. 1) is designed so that the plane formed by the optical axis of the two beams may be rotated about an axis that is equidistance from and parallel to the two beams. This capability permits the determination of the flow angularity using a "best angle" search. The procedure is to make a velocity magnitude measurement at several spot rotation angles at fixed preselected incremental steps. A plot is then made of "two spot" angular position against contrast; where contrast is defined as

$$(h - b)/\sqrt{b}$$

where h is the value of peak store of histogram (counts) and b is background (counts). A least squares fit of a parabolic equation through the maximum three adjacent points is performed and the abscissa of the parabolic vertex is taken to be the mean flow angle or best angle. Finally, the system is positioned at this angle and a velocity magnitude measurement is performed. This calculation assumes a constant particulate concentration.

For this series of tests the transceiver lens focal length was 600 mm and beam separation was 886 micrometers. The Spectron Development Laboratory (SDL) model 104 TA system has a specified accuracy of 0.1 degrees for flow angle and 0.1 m/s in velocity. Both measurements are affected by beam diameter to separation ration as well as local turbulence intensity levels in the flow field.

Wind Tunnel

The Langley 0.3 m Transonic Cryogenic Tunnel (TCT) is a single-return, fan-driven, pressure tunnel with interchangeable test sections. A 20 x 60 cm two-dimensional test section was used for this experiment. The tunnel flow is driven by a fixed-geometry single-stage fan powered by a 2.2 MW water cooled synchronous electric motor. Power is derived from a variable frequency source with fan speed from 600 to 5600 rpm. To obtain a wide range of temperatures, liquid nitrogen is sprayed directly into the stream to offset the heat added to the stream as a result of the work done by the drive fan and heat flux through the tunnel wall insulation. As a result of this direct method of cooling, gaseous nitrogen, rather than air, is the working fluid. An exhaust system which bleeds gaseous nitrogen from the low speed end of the tunnel serves as the tunnel total pressure control. The operating temperature range of the 0.3 meter TCT is from 327 K to 87 K. Mach number can be varied from 0.1 to 0.9 and Reynolds numbers as high as 55 million per foot are available within the test envelope. Further details about the tunnel are available in references 5 and 6.

Model

The model employed to produce a flow field for the LTA measurements was a 3.048 cm (1.2 in.) diameter circular cylinder which spanned the 20.3 cm (8.0 in.) two-dimensional test section. The cylinder is shown mounted in its test module in figure 2. Note the location of the "D" windows and the circular turntables which allow the window to be rotated around the model providing 360 degrees visual access. Figure 3 presents another view through one of the windows. The model is shown mounted in the test section in figure 4. Also visible in this figure is the drag rake used to obtain drag coefficient data.

The model was constructed from 15-5 ph stainless steel and heat treated (1150 modified) to provide sufficient fracture toughness for the cryogenic conditions. Although this heat treatment produces a dual phase material (austenite and martensite) which is inherently unstable and may cause model warpage, periodic checks of the model dimensions showed no indication of warpage. The surface finish specified was a rms 1.524×10^{-5} cm (8 microinches). The model contained no pressure orifices or other instrumentation.

EXPERIMENTAL SETUP

LTA Installation

Figure 5 shows the LTA laser-optics head and scan rig in place at the 0.3 m TCT. The 0.3 m TCT test section is shown with the top removed. A section of the nitrogen purge ring is visible near the plenum window. A piece of plate glass 3.81 mm (0.12 in.) thick was included in the purge arrangement. Dry nitrogen boiloff from the LN_2 tunnel supply tank was used to purge between the plenum window and the plate glass to prevent frost from forming on the plenum window. A blower directed room air across the glass plate to keep optical access to the test section clear of condensation. Optical access during earlier entries to the 0.3 m TCT had been plagued by problems of condensation and/or frost formation on the plenum window.

A 1 milliwatt helium neon laser was used to monitor the position of the LTA sample volume with respect to the cylinder. The laser was focused on a photodiode mounted on the test section turntable. Manual scan rig control based on position readout kept the system aligned during the tests as components shifted due to thermal expansion and contraction. The system was calibrated using direct measurements with an open test section.

Tunnel Seeding

Earlier entries into the 0.3 m TCT yielded data rates from the LTA system of approximately 12 correlated events per second (ref. 1). Later inspection of the tunnel circuit indicated that the particles observed were probably produced by an oil leak, which had been repaired prior to the present test. The tunnel mode of operation naturally purges the residual dust during start-up and there were no natural particulates observed with the LTA system. It was possible to introduce bursts of liquid nitrogen particles by pulsing the liquid nitrogen injection system, but they were not present during steady state operation, even at temperatures as low as 99.7 K.

To introduce particulates, service air having a dewpoint of 230 K was inbled at a tunnel temperature of 225 K to utilize the resulting condensed water vapor. Scattering events were readily detected. By varying the service air pressure, and thus the inbled mass flow rate, the data rate could be varied to any desired value. Data rates up to 3000/sec were attained, but due to concern of coating the tunnel screens with ice, the inbleeding was decreased until a constant data rate of about 100/sec was obtained. With this data rate and using 10 to 30 second integration times, excellent histograms of correlated events were obtained.

PROCEDURES, DISCUSSION AND RESULTS

Cylinder Data

The flow field of a cylinder is very complex and is sensitive to many parameters including Mach number, Reynolds number, velocity, tunnel noise, surface finish, tunnel walls, and wake blockage. Although all aerodynamic models are sensitive to these parameters to some degree, the cylinder shows a higher sensitivity than most. The circular cylinder exhibits a particularly dramatic sensitivity to Reynolds number. Another feature of cylinder flow is an open, usually oscillating, wake which is typically several cylinder diameters in thickness. Additional discussion of circular cylinder fluid mechanics may be found in reference 7. In order to monitor the flow field's behavior without interfering with the surface flow, a scanning drag rake was employed.

The drag coefficient of a cylinder is a useful parameter in many engineering applications, and may also be used as an indicator of the fluid mechanics phenomena taking place at a particular flow condition. Drag may be measured from a pitot survey of the wake as depicted in figure 6a, where the integrated decrement from free stream pitot pressure may be used to calculate drag coefficient. Mathematical details may be found in standard aerodynamics texts such as reference 8. Drag coefficient data from a scan across the wake at the midspan station of the cylinder are presented in figure 6b as a function of Reynolds number. Mach number was held constant during the scan and is constant in figure 6b. Data from an earlier test with this same model are shown qualitatively in figure 7 as a carpet plot of momentum loss, or drag, through the wake, and with the cylinder span from near the tunnel wall to beyond the center line. The plot is keyed to the location of each tube in the rake. To generate the data, the rake was traversed normal to the plane of the figure. In figure 8, a plot of change in drag coefficient with Reynolds number is also shown with three carpet plots inset to show the changes in wake thickness associated with the changes in drag. A relative thin wake of 2.4 cylinder diameters is shown in the center corresponding to the low drag region. This low drag portion of the Reynolds number range does not exhibit the wake oscillations characteristic of the rest of cylinder flow. Since the wake oscillations, aft of the cylinder could reasonably be expected to feed forward and induce a secondary oscillation in the stagnation flow, most testing was confined to the Reynolds number producing the more quiescent collapsed wake.

Stagnation Line Survey

One major objective of this tunnel entry was to make measurements along the 3.048 cm (1.2 in.) diameter cylinder model stagnation line from free-stream to the model surface. Tunnel windows did not allow measurements far enough forward of the model to measure free stream conditions. With the "D" window rotated 90 degrees from the position shown in figure 3, vertical scans were made to locate the stagnation line. This could be accomplished by searching for the location with zero flow angle, which only occurs on the stagnation line of this model. Adjustments were required to compensate for thermally induced shifts in the equipment. Data for a typical traverse are listed in Table 1. From the vertical stagnation line search U varied from 90.8 m/sec at 3.78 cm (1.5 in.) above and forward of the model to 86.5 m/sec at the stagnation line, at a point 4.43 (1.7 in.) in front of the model.

Figure 9a shows the geometry for the cylinder model scans. The horizontal scan was made along the flow direction to a point 0.32 cm (0.125 in.) from the model surface where the velocity was 34 m/sec. Figure 9b is a plot of the ratio of the velocity at each data point position to free-stream velocity as a function of x/D where x is the distance from the model surface and D is the model diameter. The 0.3 meter TCT was operating at a temperature of 225 K and a Mach number of 0.3; U was 91 meters/sec and the Reynolds number was 1.87×10^6. The circles indicate calculations based on potential theory (ref. 9) and the squares denote measurements taken with the LTA system. All errors associated with the measurements are encompassed by the size of the symbols. The data from this scan are also listed in Table 2.

The tunnel free-stream Mach number was then varied from 0.1 to 0.4 and tunnel pressure was varied from 1.93 to 3.86×10^5 N/m^2 (28 to 56 psi) to determine if the particles formed by the moisture from the service air were small enough to follow the flow. Most of the particles did follow the flow, but there was a slight skewness of the histogram on the high velocity side indicating a few of the particles were larger and did not decelerate with the surrounding nitrogen flow field.

Boundary Layer Survey

To examine the boundary layer, a vertical scan was initiated 1.4 cm (0.56 in.) from the model surface at 45 degrees from the stagnation point with the "D" window in its usual horizontal position. The LTA optic head was angled

7 degrees to the tunnel window to prevent the laser beam from impinging on the end of the model and to eliminate flare from the window surface. Tunnel conditions were $M_\infty = 0.3$, $p_\infty = 28$ psi, $R_e = 1.87 \times 10^6$ per foot and seeding was obtained by injecting service air. The data are listed in Table 3 and shown in figure 10 where velocity and flow angle are plotted as a function of distance from the model surface. If the point at which the velocity peaks is taken as the boundary layer edge velocity then the boundary layer thickness is approximately 0.19 cm (0.071 in.) thick. Beam blockage from the model and/or insufficient particle density prevented measurements closer to the surface. Scan rig control and accuracy was estimated to be 250 micrometers (0.010 in.). The boundary layer thickness is estimated to be 1.5 millimeters from the position of the velocity peak.

CONCLUDING REMARKS

Measurements were made in the flow field of a cylinder model using an LTA system in a cryogenic wind tunnel. Since natural seeding due to residual particles in the tunnel circuit was undetectable, frozen residual moisture from inbleeding of service air was used to artificially seed the flow. This provided reasonable data rates and comparison with theory indicated that the particles were small enough to follow the flow. Restricted optical access limited flow field mapping but portions of the stagnation line and boundary layer were measured. Access ports were kept frost free with a forced nitrogen purge.

REFERENCES

1. Honaker, William C.: Velocity and Flow Angle Measurements in the Langley 0.3 Meter Transonic Cryogenic Tunnel Using a Laser Transit Anemometer, NASA-CP2243, March 25-26, 1982, pp. 335-342.

2. Hunter, W. W., Jr.; Gartrell, L. R.; and Honaker, W. C.: Some NTF Laser Velocimeter Installation and Operation Considerations, NASA-CP2243, March 25-26, 1982, pp. 343-358.

3. Hunter, W. W., Jr.; Honaker, W. C.; and Gartrell, L. R.: Application of Laser Anemometry to Cryogenic Wind Tunnels, International Congress on Instrumentation in Aerospace Simulation Facilities (ICIASF), St. Louis, France, September 20, 1983, pp. 220-208.

4. Smart, A. E.; Mayo, W. T., Jr.: A Tutorial: Laser Transit Anemometry, Proceeding from the 4th International Conference on Photon Correlation Techniques in Fluid Mechanics, Stanford University, Stanford, California, August 24-27, 1980, Paper No. 2.

5. Ray, E. J.; Ladson, C. L.; Adcock, J. C.; Lawing P. L.; and Hall, R. M.: Review of Design Operational Characteristics of the 0.3 Meter Transonic Cryogenic Tunnel, NASA TM-80123, 1979.

6. Kilgore, Robert A.: Design Features and Operational Characteristics of Langley 0.3 Meter Transonic Cryogenic Tunnel. NASA TN D-8304, 1976.

7. Morkivin, M. V.: Flow Around Circular Cylinder - A Kaleidoscope of Challenging Fluid Phenomena. Symposium on Fully Separated Flows, ASME Fluids and Engineering Division Conference, Philadelphia, PA, May 18-20, 1964.

8. Schlichting, Hermann: Boundary Layer Theory. McGraw-Hill Book Company, Inc., 1960.

9. Wylis, C. R., Jr.: Advanced Engineering Mathematics. McGraw-Hill Book Co., Inc., 1951.

Table 1

Stagnation Line Search - 0.3 Meter TCT

3.05 Centimeter (1.20 Inch) Cylinder

$M_\infty = 0.3$, $P_\infty = 28$ psi, $Re = 1.87 \times 10^6$

Distance from Stagnation Line (cm)	Mean Velocity (m/s)	Flow Angle (degrees)	Data Rate (counts/sec)	Turbulence Intensity (%)
3.78	90.8	3.6	35	1.37
3.22	90.2	3.4	121	1.60
2.14	88.2	3.3	78	1.33
1.16	86.8	2.0	77	1.23
0.66	86.4	1.2	87	1.52
0.13	86.3	0.2	86	1.81
-0.34	86.6	-0.6	69	1.49
0	86.5	-0.1	122	1.40

Table 2

Stagnation Line Survey - 0.3 Meter TCT

3.05 Centimeter (1.20 Inch) Cylinder

$M_\infty = 0.3$, $P_\infty = 28$ psi, $Re = 1.87 \times 10^6$

Distance along Stagnation Line (X) (cm)	Mean Velocity (m/s)	Flow Angle (degrees)	Data Rate (counts/sec)	Turbulence Intensity (%)
4.43	86.5	-0.1	122	1.40
3.60	84.0	-0.1	132	1.88
2.78	80.0	0.0	180	3.03
1.96	72.5	-1.0	255	3.80
1.14	55.5	-0.9	311	5.50
.72	38.6	1.8	342	7.23
.32	34.0	1.4	43	4.6

Table 3

Boundary Layer Survey - 0.3 Meter TCT

3.05 Centimeter (1.2 Inch) Cylinder

$M_\infty = 0.3$, $P_\infty = 28$ psi, $Re = 1.87 \times 10^6$

Distance from Stagnation Line (cm)	Mean Velocity (m/s)	Flow Angle (degrees)	Data Rate (counts/sec)	Turbulence Intensity (%)
1.40	114.7	12.0	75	1.24
1.21	118.1	12.8	94	1.84
.96	121.8	16.0	85	1.36
.70	127.9	18.3	79	1.56
.40	137.2	24.4	84	1.50
.30	141.1	26.9	58	1.42
.22	144.1	29.4	54	1.45
.18	146.5	30.8	25	1.06
.10	136.3	30.1	50	1.95
.05	122.5	32.1	8	1.21

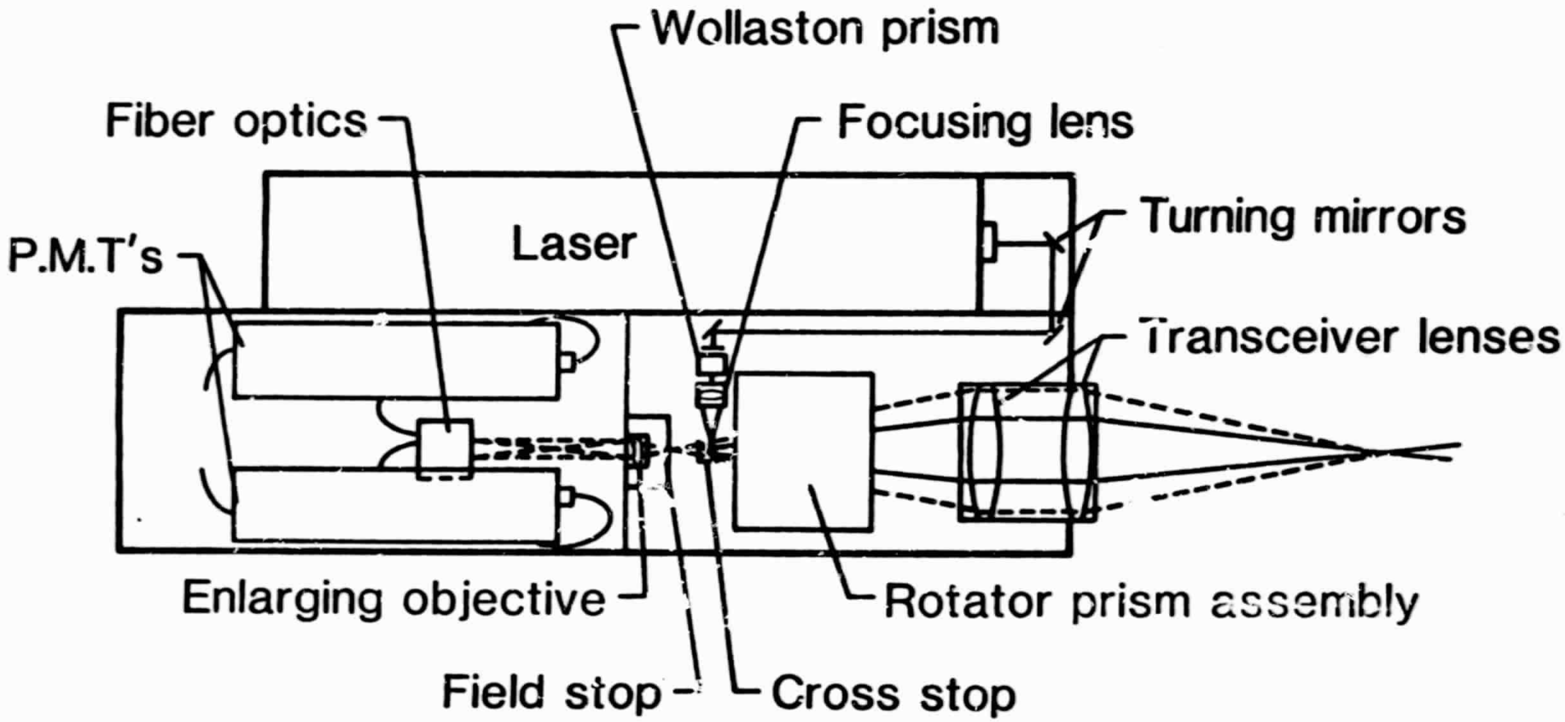

FIGURE 1. - COMPONENTS OF THE LTA SYSTEM

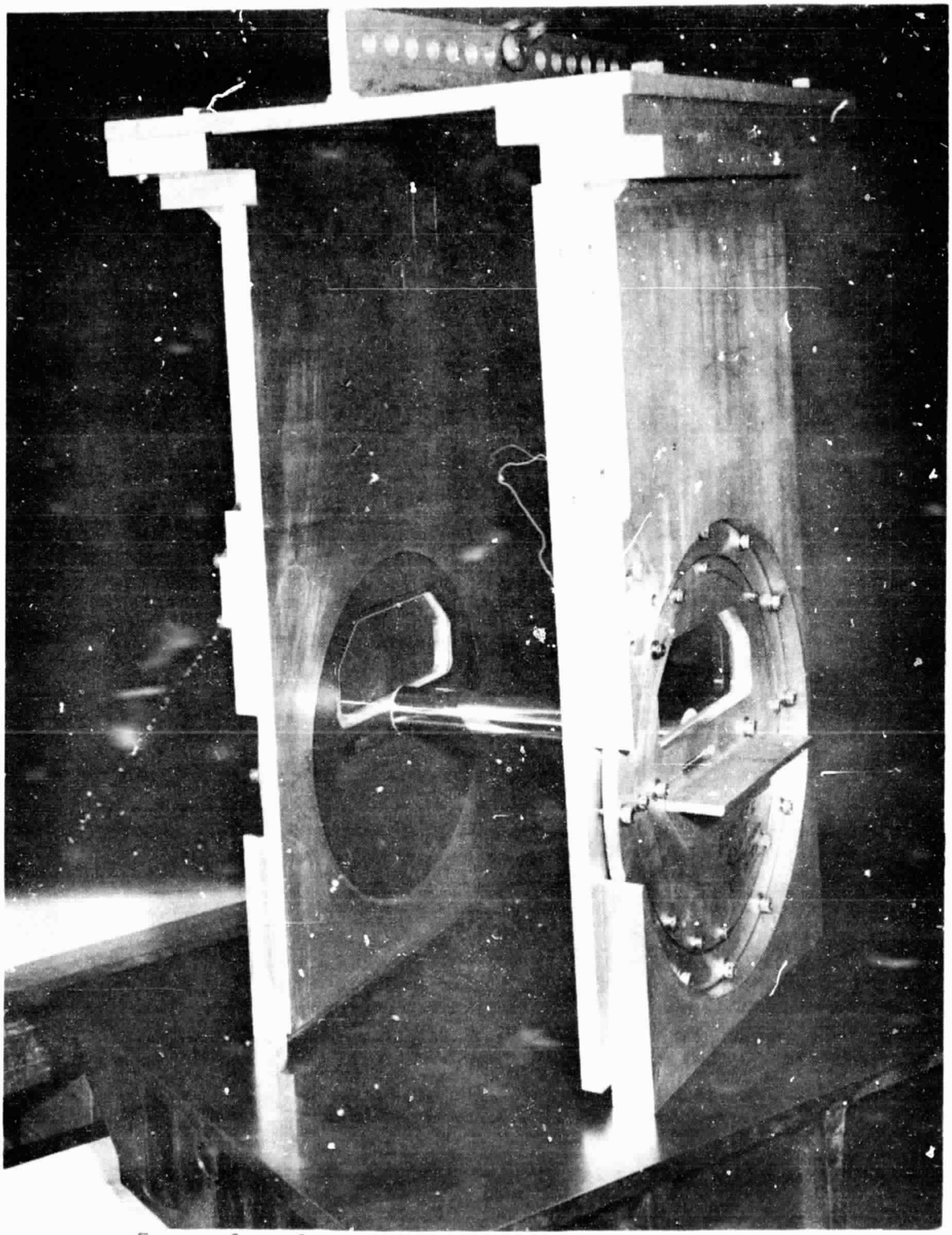

FIGURE 2. - CYLINDER MODEL MOUNTED ON TURNTABLES SHOWING THE RELATIVE LOCATION OF MODELS AND WINDOWS

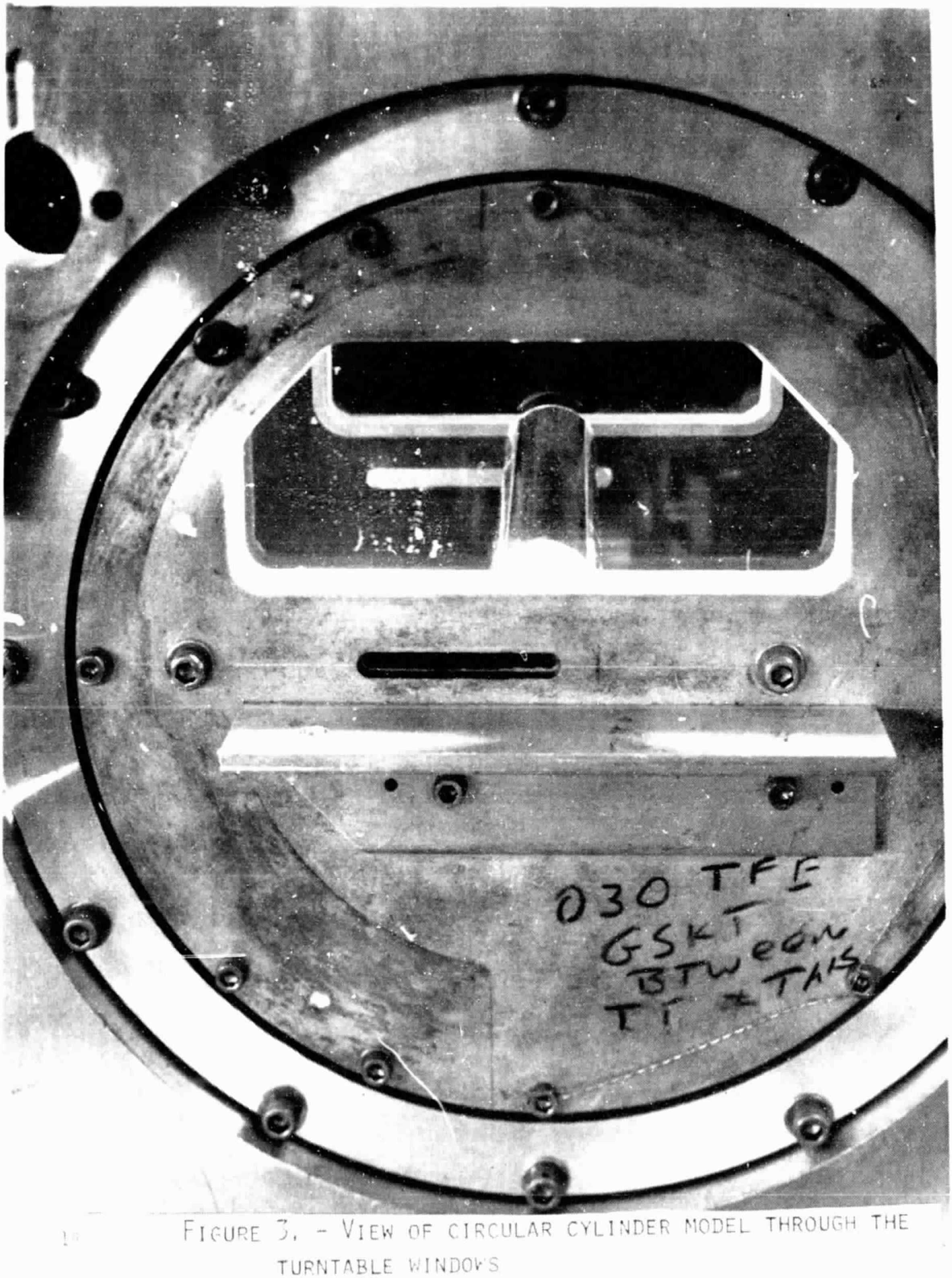

NASA
L-82 10,820

16 FIGURE 3. - VIEW OF CIRCULAR CYLINDER MODEL THROUGH THE TURNTABLE WINDOWS

NASA
L-84-2781

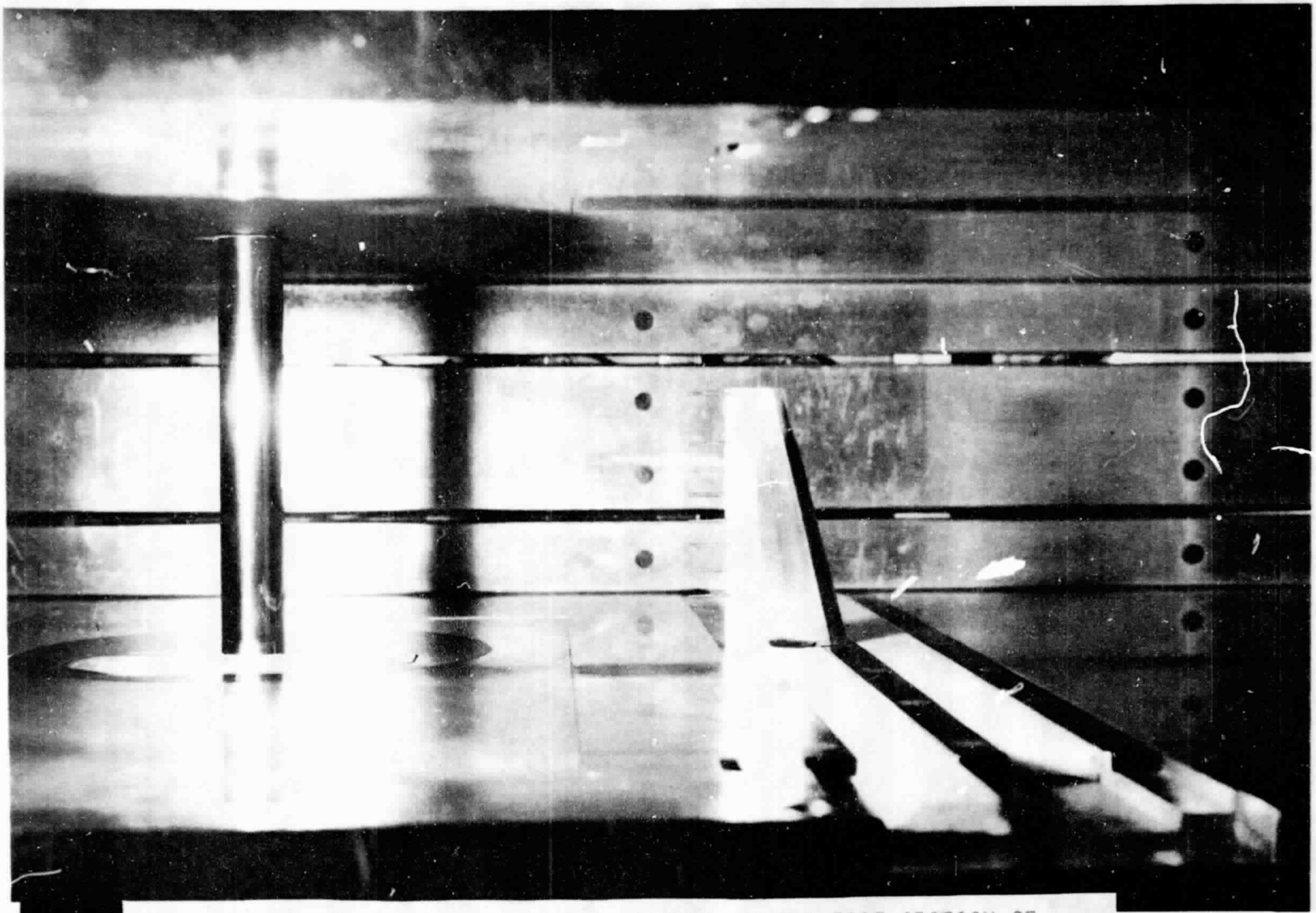

FIGURE 4. - CYLINDER MODEL AND DRAG RAKE IN THE TEST SECTION OF THE 0.3-M TRANSONIC CRYOGENIC TUNNEL

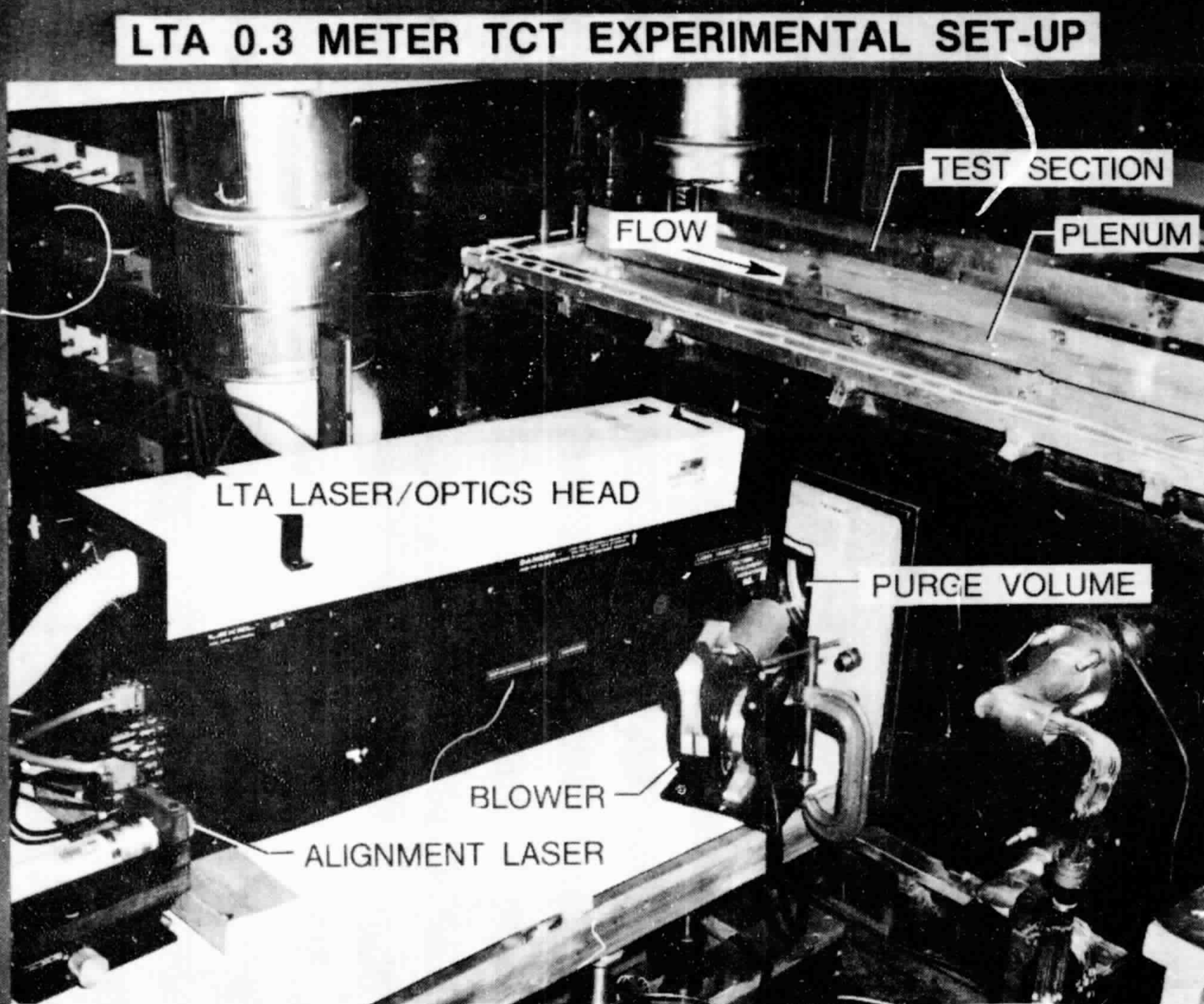

FIGURE 5. - PHOTOGRAPH OF THE LTA INSTALLATION AT THE 0.3 M TCT

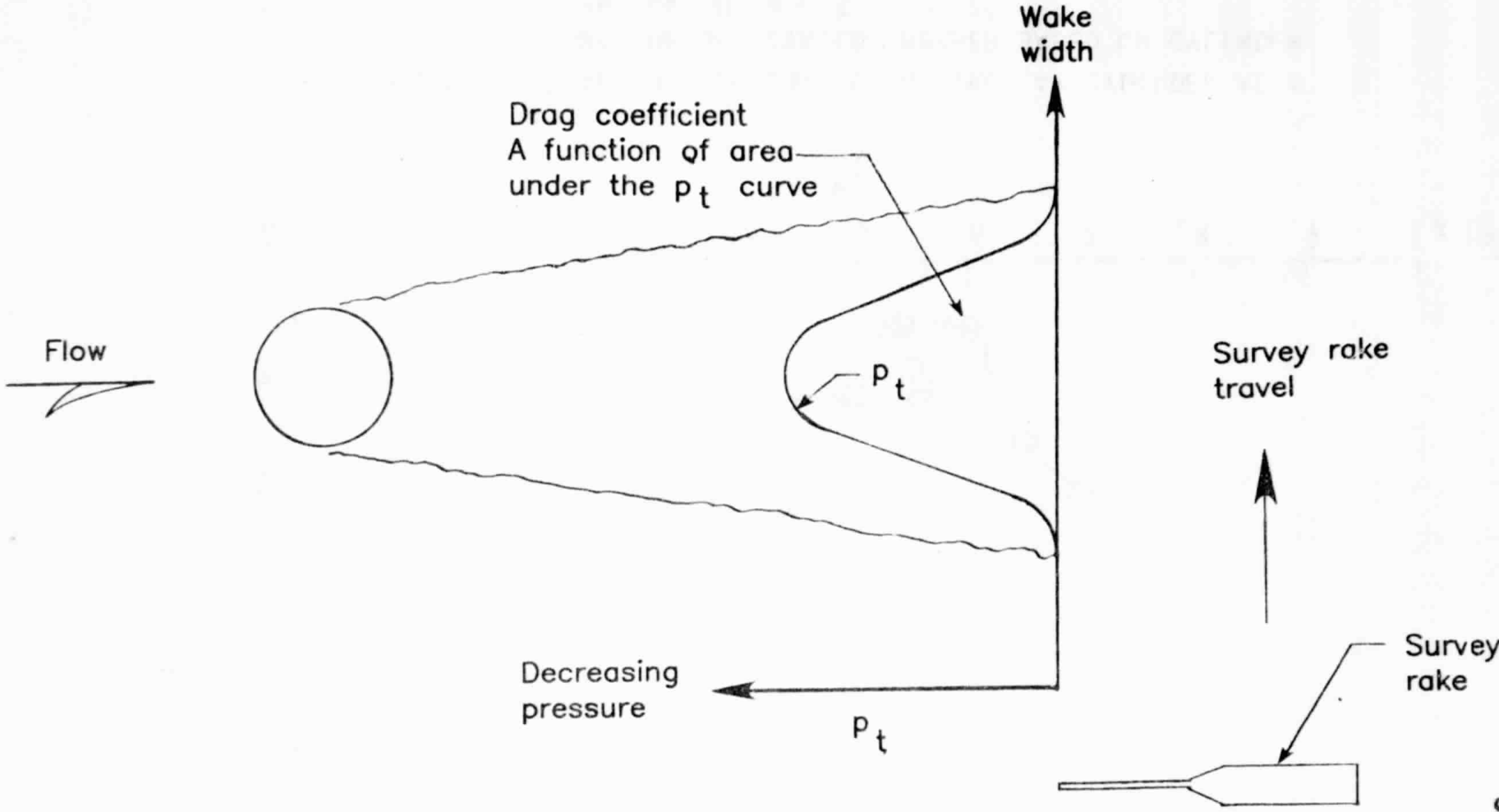

FIGURE 6A. - METHOD OF DETERMINING CYLINDER DRAG COEFFICIENT USING A SURVEY RAKE

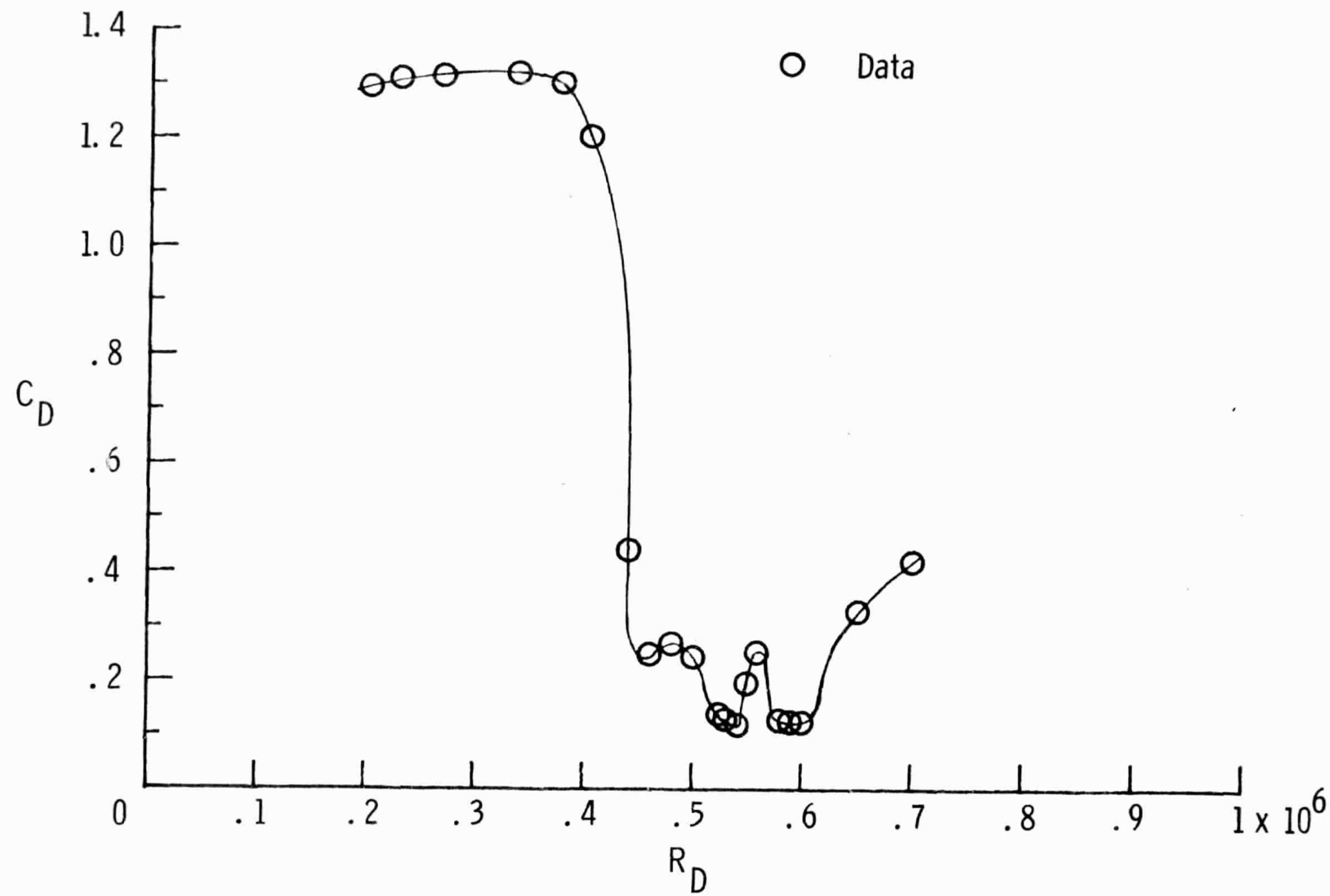

FIGURE 6B. - DRAG COEFFICIENT FOR A CIRCULAR CYLINDER AS A FUNCTION OF REYNOLDS NUMBER BASED ON CYLINDER DIAMETER, $M_\infty = 0.3$

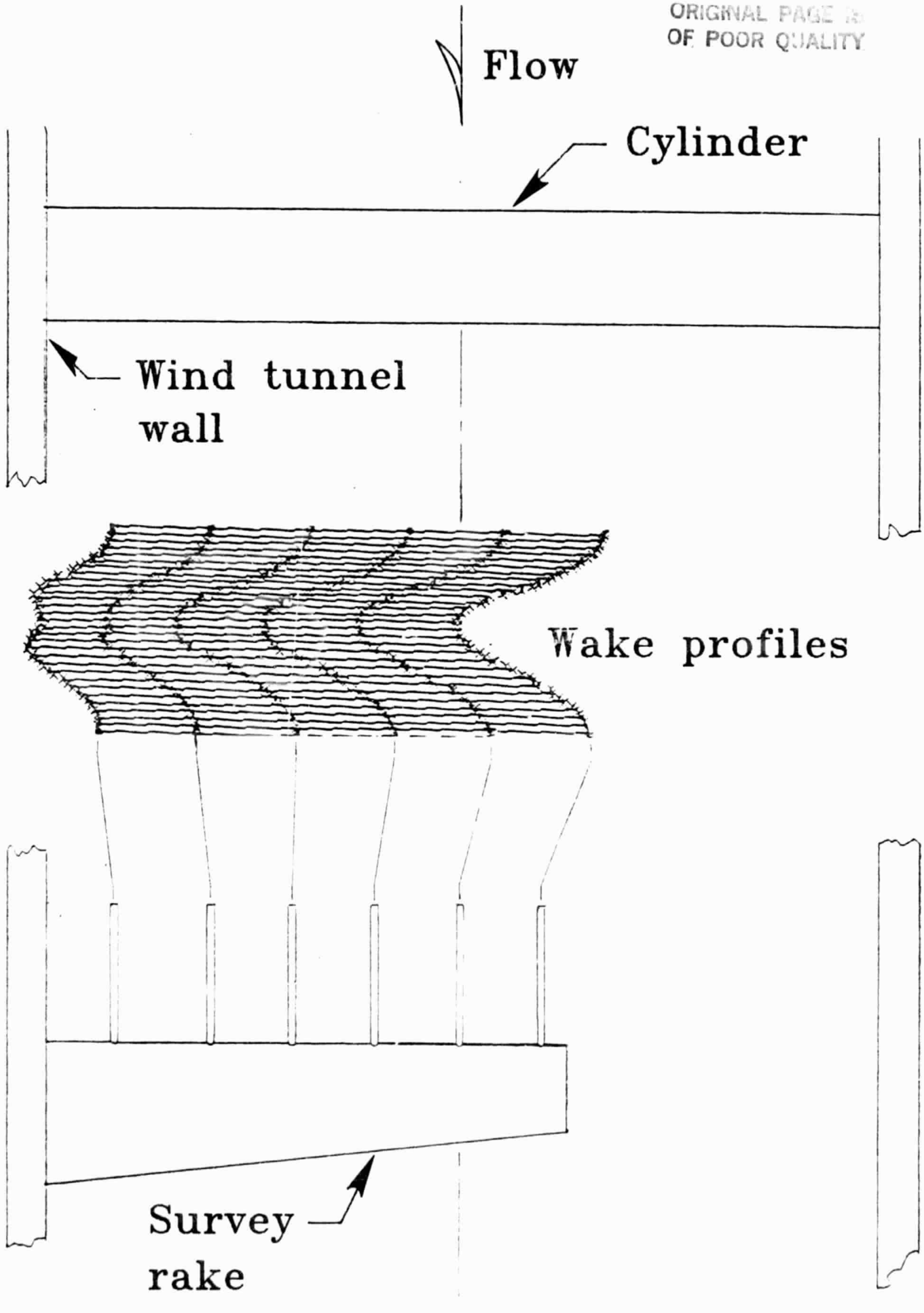

FIGURE 7. - SCHEMATIC OF DRAG SURVEY RAKE AND TYPICAL CARPET PLOT OF CYLINDER WAKE PROFILES

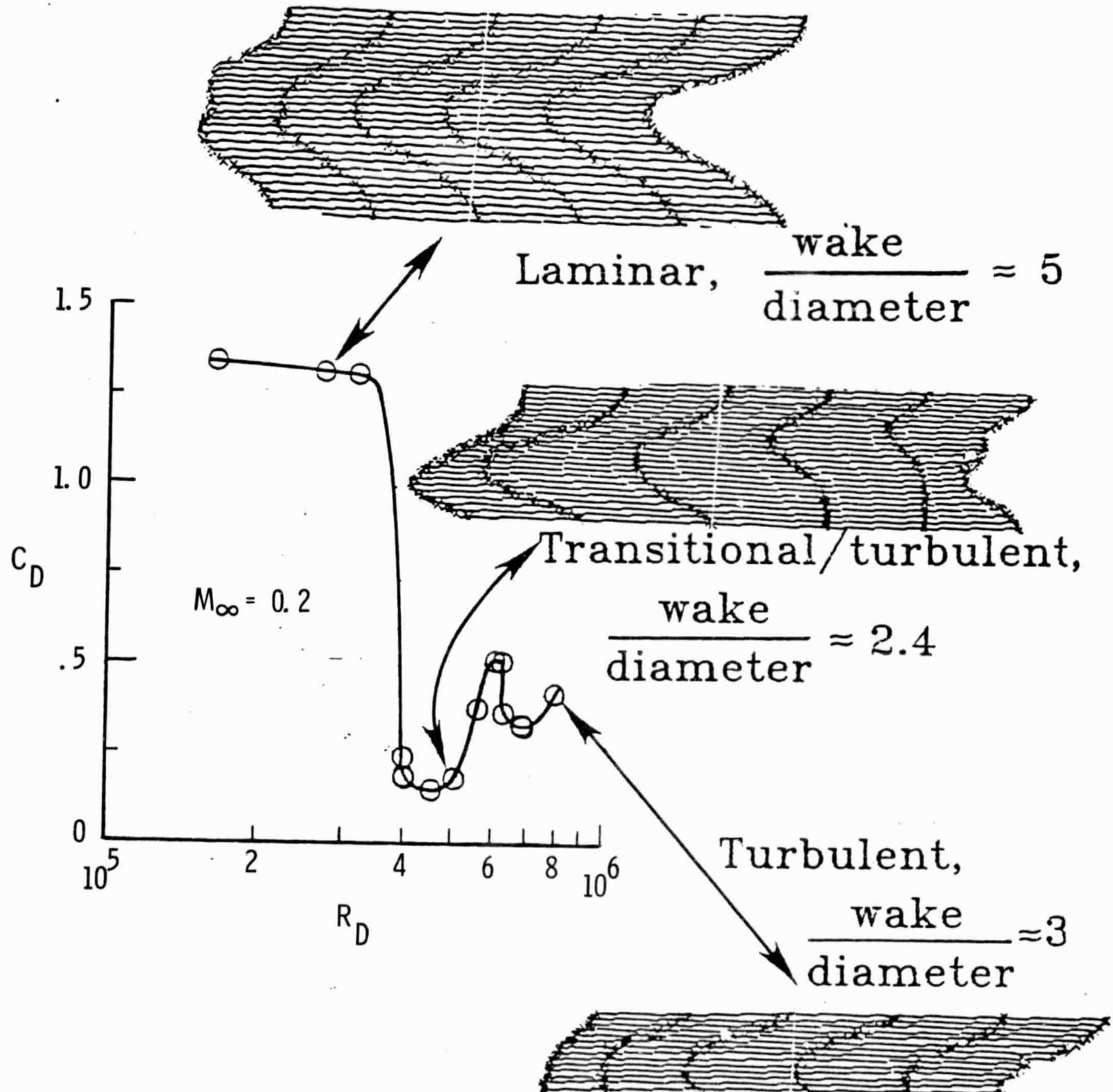

FIGURE 8. - WAKE CARPET PLOTS OF RELATIVE WAKE TO CYLINDER DIAMETER RATIOS FOR LAMINAR, TRANSITIONAL, AND TURBULENT FLOW REGIMES AT A MACH NUMBER OF 0.2

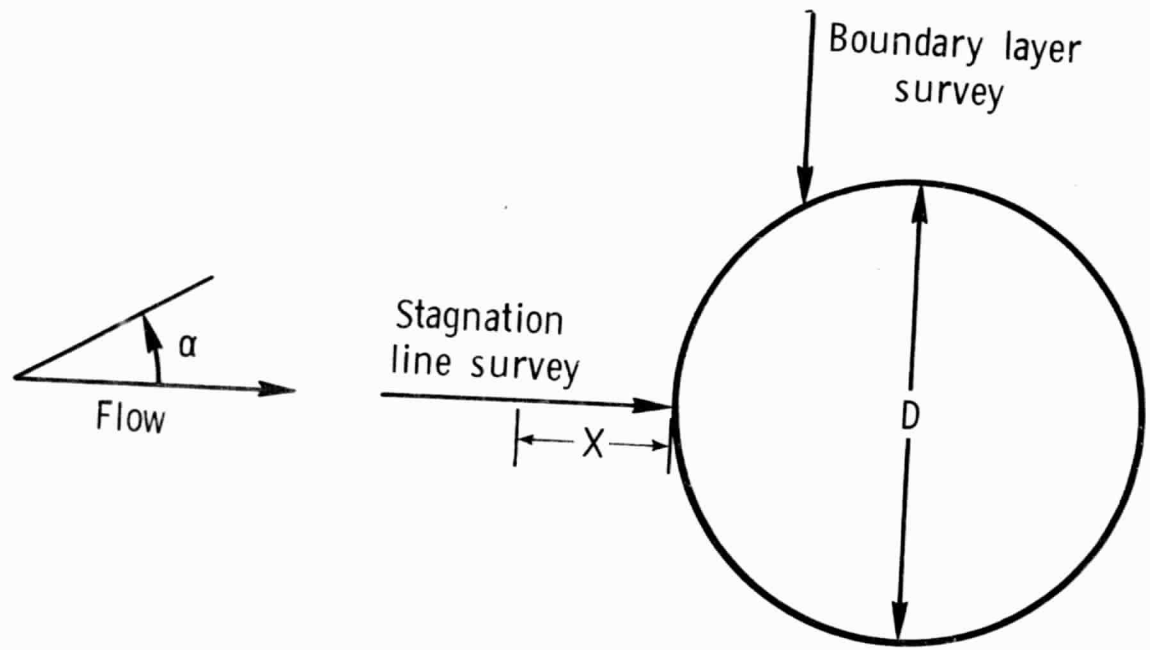

FIGURE 9A. - GEOMETRY OF LTA SURVEYS

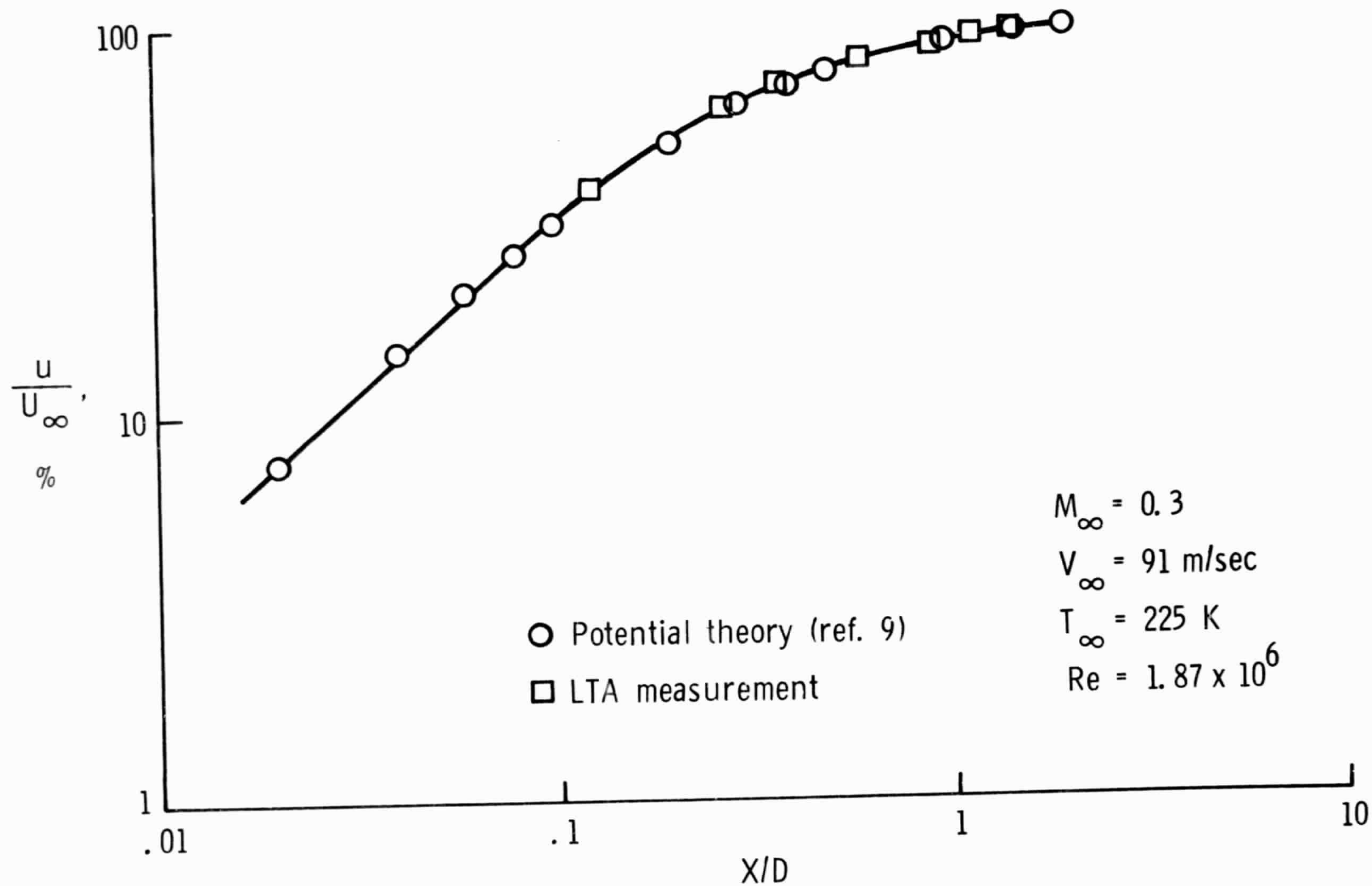

FIGURE 9B - P' 'T OF STAGNATION LINE SURVEY ON 1.2 INCH CYLINDER MODEL

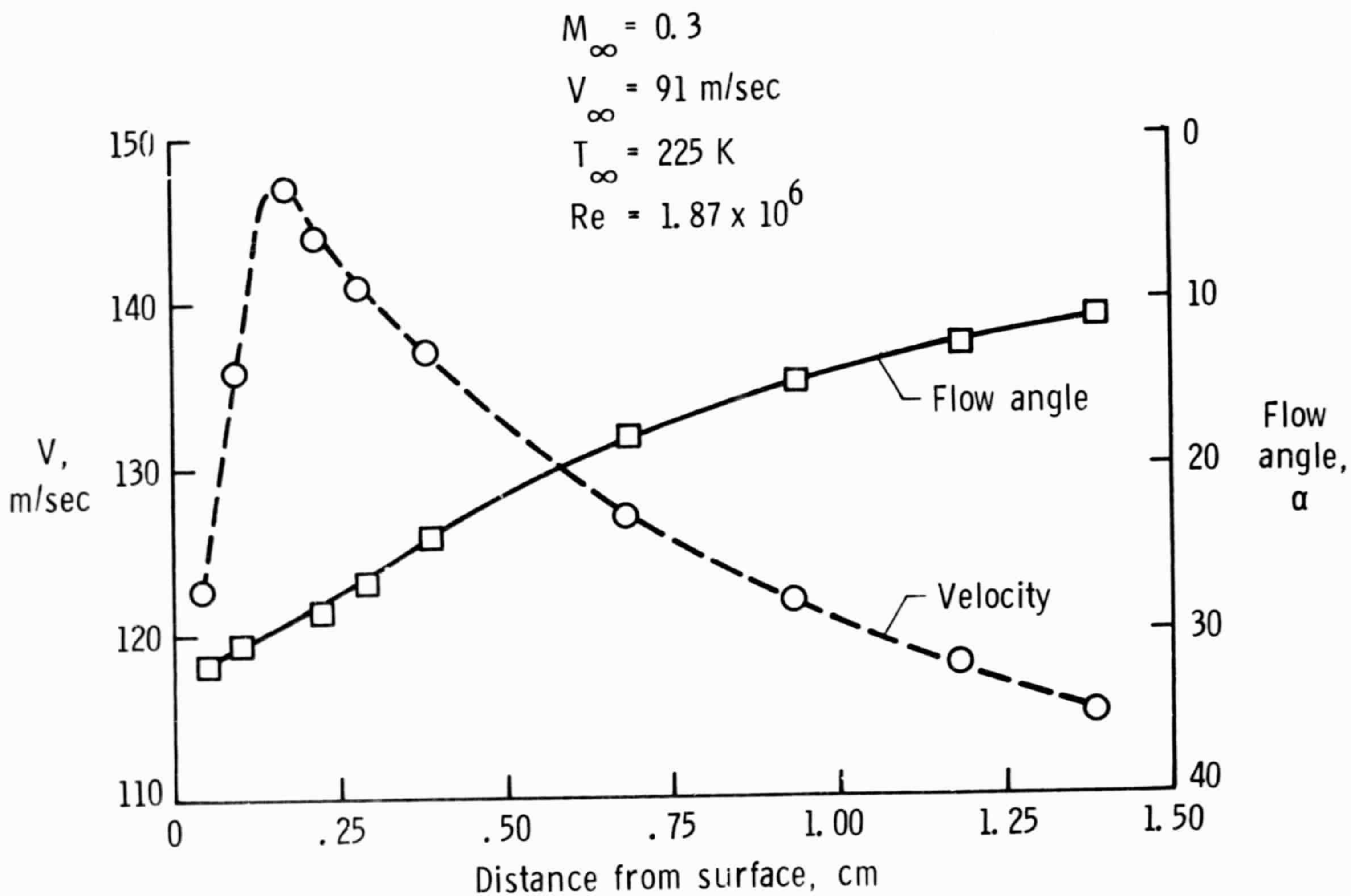

Figure 10. - Plot of boundary layer survey on 1.2 inch diameter cylinder model

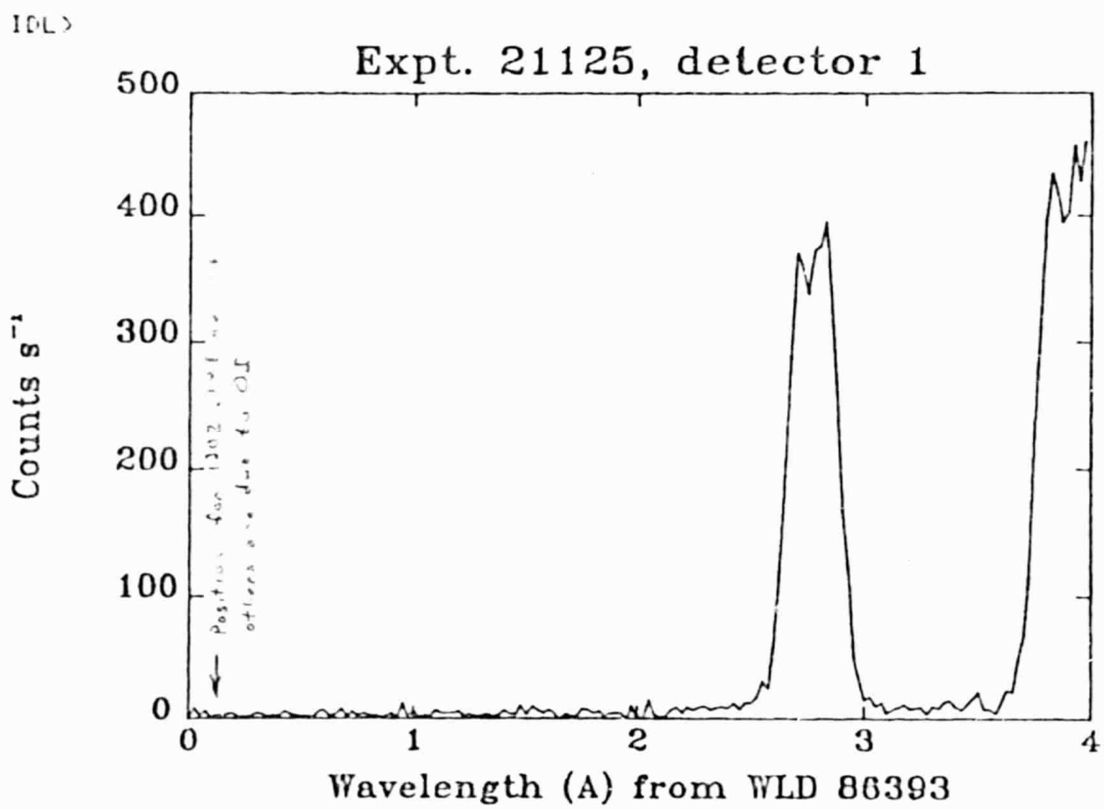
IDL>
Expt. 21125, detector 1
Counts s^-1
0
100
200
300
400
500
1
2
3
4
Wavelength (A) from WLD 86393

FIGURE 4.